 doi:10.20944/preprints202209.0056.v1

Article

Evaluating the Injection Moulding of Plastic Parts using In Situ Time-Resolved Small-Angle X-Ray Scattering Techniques

André A. Costa [1], Fábio Gameiro [1], Artur Potêncio [1], Daniel P. da Silva [1], Pedro Carreira [1], Juan Carlos Martinez [2], Paula Pascoal-Faria [1], Artur Mateus [1] and Geoffrey R. Mitchell [1,*]

[1] Centre for Rapid and Sustainable Product Development, Polytechnic of2430-080 Leiria, Portugal; andre.a.costa@ipleiria.pt (A.A.C.); artur.c.potencio@ipleiria.pt (A.P.); fabio.a.gameiro@ipleiria.pt (F.G.); daniel.p.silva@ipleiria.pt (D.S.); pedro.s.carreira@ipleiria.pt (P.C.); paula.faria@ipleiria.pt (P.P.F.); artur.mateus@ipleiria.pt (A.M.)
[2] NCD-SWEET beamline, Alba Synchrotron Light Source, Cerdanyola del Vallès, Barcelona, Spain; guilmar@cells.es (J.C.M)
* Correspondence: geoffrey.mitchell@ipleiria.pt

Abstract: We describe the design and fabrication of an industrial injection moulding system which can be mounted and used on the NCD-SWEET Small-angle X-Ray Scattering Beamline at ALBA. We show how highly useful time-resolved data can be obtained using this system. We are able to evaluate the fraction of material in the mould cavity and identify the first material to solidify and how this varies with the injection temperature. The design follows current industrial practice and provides opportunities to collect time-resolved data at several points within the mould cavity so we can build up a 4D perspective of the morphology and its temporal development. The quantitative data obtained will prove invaluable for the optimisation of the next generation of injection moulding techniques. This preliminary work used results from the injection moulding of a general purpose isotactic polypropylene.

Keywords: Injection moulding; Crystallisation; Flow; Small-angle X-ray Scattering; isotactic polypropylene

1. Introduction

Injection moulding is the most common technology employed to fabricate parts from polymers [1]. In this, a polymer in the softened or molten state is injected, at high pressure, into a shaped mould, usually manufactured in metal and held at room temperature or an intermediate temperature. As a consequence, the polymer cools and becomes solid either through a glass transition or a crystallization process. Semi-crystalline polymers such as polyethylene and polypropylene are the most widely used, and the time profile of temperature and flow have a major impact on the properties of the final part [2]. The presence of flow, inherent in the injection moulding process, means that the final product does not show the typical spherulitic morphology of crystallisation from a quiescent melt [3]. In the case of crystallisation of a melt subject to flow [4], the longest chains of the polymer melt will become extended and this will serve as row nuclei for the unstressed chains in the polymer melt which leads to a high level of preferred orientation due to the common alignment of the extended chains. Of course the generation of a highly aligned morphology depends on whether the extended chains have relaxed back to an isotropic configuration and this will depend on the molecular weight

 doi:10.20944/preprints202209.0056.v1

distribution of the polymer. In the standard tube model of rheology, the relaxation time for a chain constrained in a tube scales with the molecular length squared. All of these factors means that the morphology which develops during injection moulding involves an interplay of cooling rates, flow conditions and relaxation. For those reasons, the development of the morphology has a history, and some post-moulding experimental techniques, such as electron microscopy of differentially etched samples [5,6], in skilled hands can unravel the history.

Traditionally, crystallization and flow are studied with laboratory equipment and the post-moulding analysis of samples prepared using injection moulding. In the last 30 years, synchrotron-based small-angle (SAXS) and wide-angle X-ray scattering (WAXS) [7] have greatly enhanced our understanding of polymer crystallization using in-situ time resolving techniques and where appropriate, flow stages, such as shear cells [8,9,]. SAXS techniques have the capability to quantify the development of crystals and the level of preferred orientation [6]. Now, as outstanding as this work was, it had limited direct relevance to injection moulding due to the extreme cooling rates and the interwoven flow fields, present in the mould. We reviewed all of the possible time-resolving quantitative techniques and identified that synchrotron SAXS techniques provided the only practical technique which could be used. These provide quantitative data on the relevant structural scales, the energy of the x-rays means that relevant sample thicknesses could be used and they do not require optical transparency, the small diameter of the incident beam means that data is obtained relevant to a specific point, and mapping an area would be straightforward and the small volume of the incident and scattering beams resulted in a simple design strategy. When we reviewed the literature, we found few relevant publications, some had employed WAXS techniques [10,11] which have different requirements to SAXS with the moulding of liquid crystal polymers. The most relevant work was on micro-injection moulding and on injection moulding with metal moulds and x-ray transparent diamond windows [12,13]. Diamond windows are widely used in high pressure cells for x-ray scattering [14], but of course they give access to only a small part of the mould cavity. We identified these publications as very interesting work but which was focused on developing a scientific understanding, rather than reflecting industrial practise.

This work is focused on addressing this matter to design, manufacture and test an injection moulding system, which is designed to be relevant to current and as far as possible future industrial practice.

2. Materials and Methods

The design of an injection moulding system to mount on the selected beamline [15] must meet the geometric and weight limitations of the beamline and its components. After consideration of the various options, we selected an Industrial Autonomous Injection Unit, UAI6/1OP from the Rambaldi Group which consolidates most of the control and power components and the remote control in a floor mounted unit. The mould and clamping systems were designed by ourselves. The mould cavity is manufactured from standard

 doi:10.20944/preprints202209.0056.v1

mould components, mould plates and mould inserts and uses industrial-scale recirculating heating and cooling units units to maintain a constant temperature.

The beamline mounted injection moulding system is shown in Figure 1 mounted on the NCD-SWEET SAXS Beamline at the ALBA Synchrotron Light Source, which is equipped with a DECTRIS Pilatus3S 1 M detector system mounted 6.7m from the sample and an incident wavelength of 1Å. The Pilatus Detector system is built up of an array of silicon sensors equipped CMOS electronics. As a consequence, a small portion of the detector is not active (~7%) which appear as black stripes in the recorded intensity images. The charge induced by the X-ray photons is detected and processed by the pixel readout system. This detector has an effective pixel size of 172 x 172 micrometres and a dynamic range of 20 bits. SAXS patterns were recorded over a q-range from 0.002 $Å^{-1}$ to 0.125 $Å^{-1}$ where $|\underline{Q}| = 4\pi \, Sin\theta/\lambda$, 2θ is the scattering angle and λ is the incident wavelength. Although we employ a fixed geometry with a flat detector, the small scattering angle means that the scattering vector lies in the plane of the mould cavity and so the complete azimuthual range of data, $\alpha = 0$ to $360°$ is available, where α is the angle between the scattering vector $\underline{Q}$ and the flow axis in the mould cavity. To prevent saturation of the detector by the zero angle X-ray beam, a beam stop is placed in front of the detector to absorb the transmitted beam. The detector orientation and sample to detector distance were calibrated using the well-known standard silver behenate [16].

This work was focused on the moulding of isotactic polypropylene, specifically a LydoellBasell Polypropylene MOPLEN HP500N which is a general purpose polypropylene suitable for food contact applications. It exhibits a melt flow index (MFI) of 12 g/10 min at 230°C. The injection moulding system has a minimum charge of pellets for a successful operation of ~12 g, which makes the system particularly suited for research and development of new materialsThe CT scans of the mould inserts were obtained using a Nikon XT H 225 ST 2X Industrial Scanner.

The x-ray beam paths, both the incident beam and the scattered signal, are a critical part of the injection moulding system.. There are competing factors of X-Ray transparency, and thermal conductivity together with mechanical strength to withstand the pressure in the mould which is may reach 1600 Bar.

There have been relatively few systems reported in the literature and one approach has chosen to reconcile these competing requirements by opting for a metallic mould with x-ray transparent windows in the form of diamonds [12,13]. This is a well-established approach widely exploited in the design of x-ray cells for high-pressure studies [14]. We note one of the key differences between a high-pressure stage and an injection moulding cavity is the scale of the active volume and the need to probe the behaviour of the polymer throughout the cavity.

We have opted to follow an alternative approach which maintains the current mould design practice while introducing a high level of x-ray transparency. This is a development of the approach employed by Rendon et al [11]. Figure 2 shows the CT scan of the mould insert used to define the cavity.

 doi:10.20944/preprints202209.0056.v1

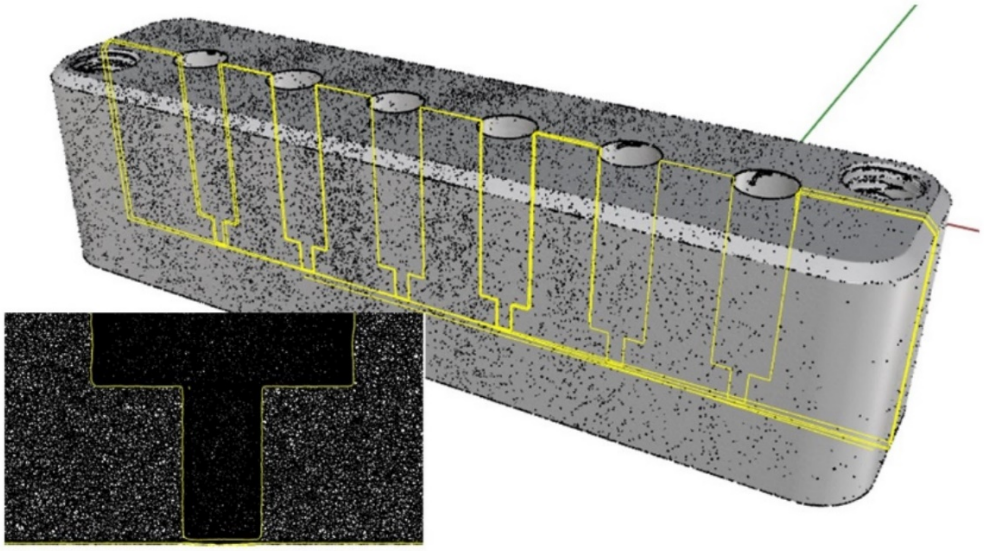

Figure 1 An X-ray CT of one of the mould inserts used in this work. The insert shows an enlarged image showing the thin "window" are at the base of each blind hole

These inserts are made of a standard insert material, an aluminium/silicon alloy AW6082. Six blind holes were introduced into the two mould inserts. Initially the hole had a diameter of 5 mm and close to the other face the hole was narrowed to 1.5 mm to minimize the area of the “window” and the hole was stopped ~0.1mm from the other surface. The CT image confirmed the expected results and the thickness of the 12 “windows” were measured as 0.0832 mm with a standard deviation of 0.0015 mm. This gives an attenuation for the two inserts of < |30|% for 12.4keV photons. Changes to the cavity geometry or the thermal characteristics can be quickly introduced by replacing the inserts. They are located in a precision engineered slot and retained using screws. . The hardening of the aluminium alloy from which the inserts were made was studied by Rowolt et al. [17]. The temperature cycle which the inserts experience during the injection moulding experiments will not affect the level of precipitation in the alloy which could alter this “background scattering”.

 doi:10.20944/preprints202209.0056.v1

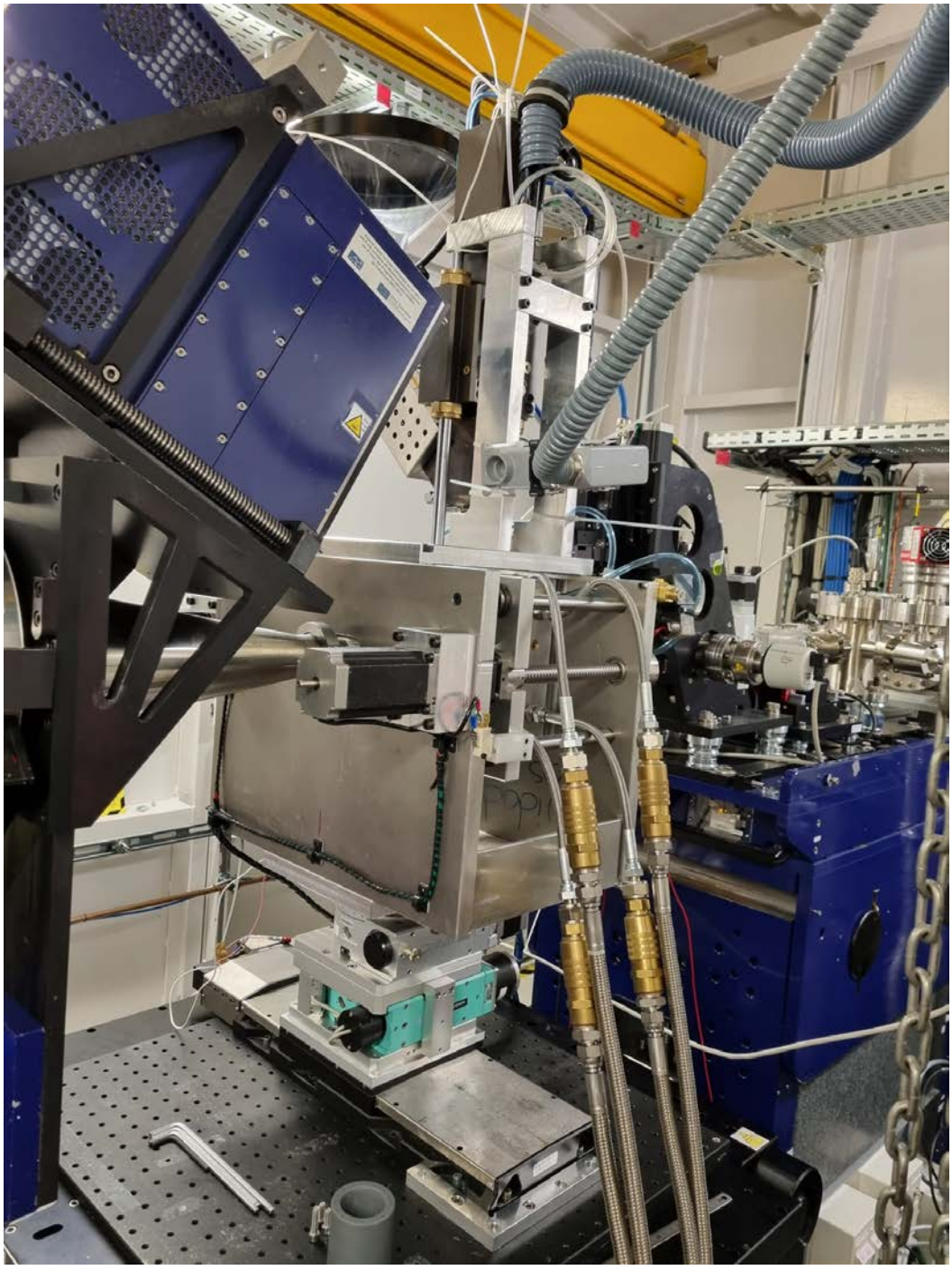

Figure 2 The injection moulding system developed in this work mounted on the NCD-SWEET Beamline. The incident beam enters from the right and the small-angle x-ray scattering detector is mounted 6.7m to the left and is connected via a vacuum tube which has a conical front piece which is located very close to the exit side of the mould. The dark blue box which can be observed just above the vacuum tube is the wide-angle x-ray scattering detector which was not used in this experiment.

3. Results

Preprints (www.preprints.org) | NOT PEER-REVIEWED | Posted: 5 September 2022 doi:10.20944/preprints202209.0056.v1

The injection moulding system was successfully mounted on the NCD-SWEET Beamline (Figure 2). The system was aligned with respect to the incident x-ray beam using the xyz translation stage in conjunction with a diode which measured the incident x-ray intensity in front of the beam stop. The injection moulding system was also mounted on a rotational stage and this proved invaluable fo aligning the relatively long and narrow pathway through the mould. After alignment we then measured the scattering from the empty cavity. This was as expected. It exhibited a well-defined isotropic pattern centered around the beam stop (Figure 3a) typical for an aluminium/silicon alloy which forms the window material. Figure 3b shows the azimuthually averaged data. This scattering can be easily subtracted from the experimental patterns when the mould contains the polymer. It is clear that the alignment of the system was very good and there no signs of any specular reflection from the incident beam hitting the side of the blind holes in the mould inserts. The alignment of the systems was stable when the mould was opened and closed and also when polymer was injected under pressure in to the mould.

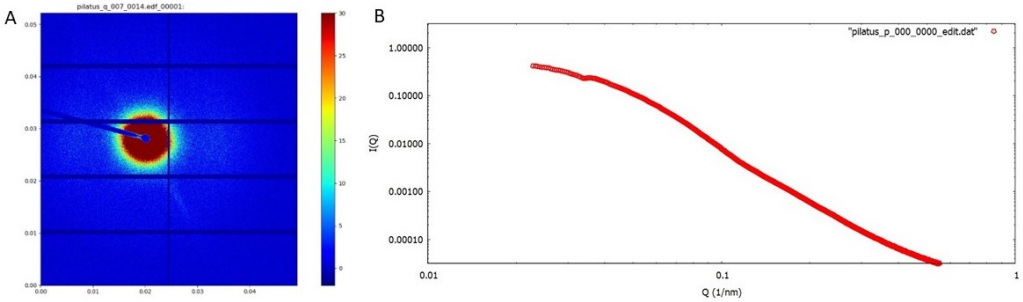

Figure 3 (a) the SAXS pattern for the empty mould cavity. The SAXS detector over the range in Q from 0.002 to 1.25 nm^{-1} (b) The azimuthually averaged data shown in Figure 3a. plot on a log-log scale

All of the equipment worked according to plan including the remote control of the injection moulding system and the ejection of the part. We were able to observe remotely in real-time the temperature and pressure in the mould. A part could be produced on a cyclic basis using the remote control. Each of the 6 windows allows the development of the morphology to be evaluated at different points in the mould cavity.

Table 1 Operational modes of Multi-window Mould

Mode	Number of data points per sampling point	Time between pts at a sampling point (s)	Data Accumuation Time (s)

 doi:10.20944/preprints202209.0056.v1

A	300	1	1
B	25	18	1
C	Variable	Variable	1

We are able to identify three types of experiments (Table 1). The first type, Mode A involves positioning the beam at one of the windows, for example window 1 and recording a time-resolving sequence of small-angle x-ray scattering patterns from before the start of the injection process to the completion of the moulding cycle. The second type of experiment, also uses Mode A,to use a similar sequence for a succession of equivalent moulding cycles, but with the incident x-ray beam positioned in turn at each of the windows. In such an arrangement we rely on the reproducibility of the injection moulding cycle so that we sample different points in the cavity in different moulding cycles. Alternatively we could relatively move the incident beam during one cycle to different windows, but the movement time would reduce the amount of scattering data recorded for each cycle. One version of this is Mode B, but we could tailor the sampling points and sequences optimised to yield specific data (Mode C). During each data accumulation, we can measure the transmission of the cavity using a diode placed in the beam-stop and this enables the fraction of material, whether molten or solid in the mould cavity to be evaluated. In the experiments reported here we focus on time series of patterns recorded for a particular window, multiple window experiments will be reported in a later publication after the required experiments. We note here that the position of the sampling ports can be adjusted for a particular mould cavity or processing parameters by preparing a set of mould inserts with different port positions guided, for example by computer simulations.

In Figure 4, we show SAXS patterns obtained using Mode A with sampling position 1, that is the position closest to the injection point. Figure 4a shows the sequence of SAXS patterns recorded 10s after injection of the polypropylene at 250°C. The mould temperature was held constant throughout these experiments at 50°C. The first pattern in Figure 4a is that of an empty cavity. As we move to the right in this sequence, we observe the emergence of a circular ring of scattering. The pattern is typical for a semi-crystalline polymer in which crystallisation has been nucleated in a quiescent melt and the chain folded lamellar crystals in random orientations. The intense peak can be used to evaluate the long period and the azimuthal variation in intensity, the level of preferred orientation of the lamellar crystals, in this case zero. We use the azimuthal variation of intensity as a function of α and a fixed value of $|\underline{Q}|$ corresponding to the peak maximum.

Preprints (www.preprints.org) | NOT PEER-REVIEWED | Posted: 5 September 2022 doi:10.20944/preprints202209.0056.v1

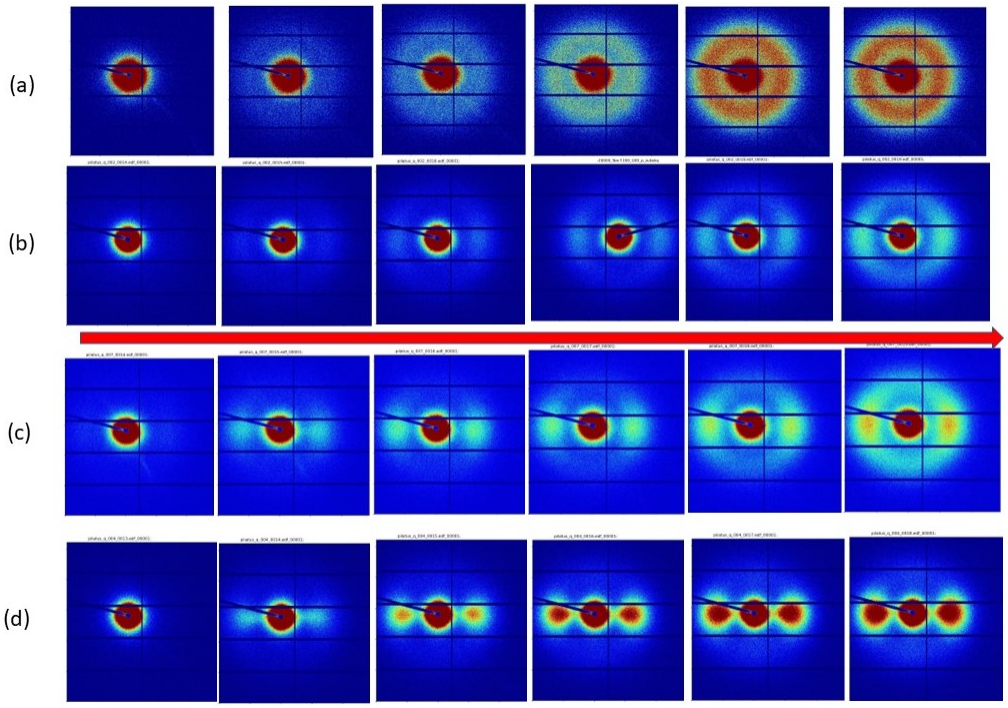

Figure 4. SAXS patterns obtained at approximately 1s intervals at the first viewing port for injections at (a) 250 ℃, (b) 210 ℃, (c) 205 ℃, (d) 190 ℃. The flow in the mould cavity is horizontal as indicated by the horizontal arrow. Time increases from left to right. The intensity mapping is constant within each sequence. The horizontal and vertical dark lines correspond to insensitive areas in the detector as it is made up of rectangular elements. The dark spot in the centre of the pattern corresponds to the area of the detector blocked by the beam stop and the angled black line corresponds to the mount for the beam stop. The SAXS detector cover the q-range from 0.002 Ă-1 to 0.125 Ă-1. The data shown here is the raw experimental data, no background has been subtracted so that the quality of the data may be easily judged.

The sequence of patterns shown in 4d is very different to those in Figure 4a, and show the development of a highly anisotropic pattern in which the intensity is greatest in the direction parallel to the long axis of the mould cavity and to the direction of flow within that cavity. These patterns were recorded for an extrusion temperature of 190°C and a constant mould temperature of 50°C. The pattern is typical for a semi-crystalline polymer in which crystallisation has been nucleated in the melt by row nuclei and the chain folded lamellar crystals have grown out normal to the row nuclei and therefore to the flow axis [18]. The very high level of orientation is a consequence of the alignment of the extended chains which form the row nuclei, which will have a common axis of alignment throughout the sample in this central zone of the mould cavity. As we progress in time, we see the development of greater fraction of crystals all of which have the same very high level of preferred orientation. We need to remember that the material will crystallise even under quiescent conditions, albeit at a slightly low temperature. In this case, all of the crystals have been templated by the row nuclei and that the density of row nuclei is sufficiently high that chain folded lamellar crystals growing out from the row nuclei impinge and fill space before the directing influence of the

Preprints (www.preprints.org) | NOT PEER-REVIEWED | Posted: 5 September 2022 doi:10.20944/preprints202209.0056.v1

row nuclei is lost. The work of Bassett [19], shows elegantly that the directing influence can extend over 1µm in the case of polypropylene. Wangsoub et al. [20] have developed a simple model to predict the overall level of preferred orientation of the polymer for an equivalent system in which the row nuclei are formed from self-organisation of a low molecular weight additive based on templated zone and isotropic regions of crystallisation.

We note that the sequences of SAXS patterns shown in Figure 4 are not the most useful display of the data, and what would be more helpful if we could present the SAXS patterns which correspond to the crystallisation in each 1s frame, in other words we need to unravel the accumulated data shown and separate into the scattering for the first 1s and the second 1s, etc. We are developing a methodology to achieve this which exploits the particular characteristics of a series of spherical harmonics to represent the data in way which separates the orientational aspects from the Q dependence features using an approach already established for multiple component systems [20].

The 2d SAXS pattern I(Q,α) is a convolution of the scattering for a perfectly aligned sample $I^0(Q,\alpha)$ and the orientation distribution of the lamellar crystal orientation D(α) [11]. The Legendre Addition Theorem allows us to write this convolution as the product of the amplitudes of a series of spherical harmonics for each of these three functions [20,21].

$$I_{2n}(|\underline{Q}|) = \left\{\frac{2\pi}{(4n+1)}\right\} D_{2n} I^{0}_{2n}(|\underline{Q}|),\alpha) \qquad \text{(Equation 1)}$$

Where $I_{2n}(|\underline{Q}|)$, $I^0_{2n}(|\underline{Q}|)$ and D_{2n} are the spherical harmonic series representing the experimental scattering I(Q,α), the scattering for a perfectly aligned system, and the orientation distribution of the normal to the chain folded lamellar crystals. Only the even order coefficients are required as a consequence of the presence of an inversion centre in the scattering pattern for a weakly absorbing sample [21]. The coefficients for the scattering of a perfectly aligned system have been derived by Lovell and Mitchell [21]. We can write the global orientation parameters $\langle P_{2n} \rangle$ as [20]:

$$< P_{2n} >_Q = \frac{1}{(4n+1)P_2^m} \int_0^{\pi/2} \frac{I(|\underline{Q}|,\alpha) \sin\alpha P_2(\cos\alpha)\, d\alpha}{I(|\underline{Q}|,\alpha) \sin\alpha\, d\alpha} \qquad \text{(Equation 2)}$$

The orientation parameter $\langle P_2 \rangle$ is the first component of an even series which describes the orientation distribution function of the normal to the lamellar crystals, Representing the data as a series. If $\langle P_2 \rangle = 0$ the distribution is isotropic, if $\langle P_2 \rangle = 1$ the crystals are arranged with the same perfect preferred orientation [11].

The objective of this work is to be able plot the level of preferred orientation of the crystals which have formed in each 1s time period after injection has commenced. This will allow us to separate out the two processes taking place in the sequences shown in Figure 4. One is the increasing fraction of crystals formed and the other is the changing level of preferred orientation of those crystals. This will allow us to extract the most information from the availability of the in-situ time-resolved SAXS data which will help unravel some of the complexity of morphology formation in injection moulding.

Conclusions

This project has focused on designing, fabricating and validating an injection moulding system for plastics which will fit on and operate with the ALBA NCD-SWEET Beamline but which conforms to current industrial mould design practice. The use of mould inserts with localized thin windows leads to an attenuation of the primary x-ray beam, with 12.4keV photons of less than 30%, We show that we are able to use this system to mould samples of isotactic polypropylene at a range of injection temperatures which gives rise to a reducing level of preferred orientation of the chain folded lamellar crystals with increasing injection temperature.

By performing these experiments in-situ we are able to separate out the different stages of crystallization in the mould and their variation with injection temperature. The design of the mould cavity and the sampling points will allow the morphology to be measured along the fill path of the mould in future work and we will be able to create a 3D model of the development of morphology under industrially relevant conditions with industrially relevant polymers.

Author Contributions: conception, GRM, PPF, AM; methodology, AAC,AP, JCM, FG, PC, AM, DS, GRM; software, GRM.; validation, GRM.; formal analysis, ; investigation, AAC,AP,FG, DS,PC,AM, GRM, JCM; resources, GRM,AM,PPF; data curation, GRM; writing—original draft preparation, GRM,AC ; writing GRM, PPF,AAC, AM ; visualization, GRM.; supervision, GRM AM, PFF; project administration, GRM PPF; funding acquisition, GRM, PPF, AM. All authors have read and agreed to the published version of the manuscript

Acknowledgements

These experiments were performed using the NCD-SWEET beamline at the ALBA Synchrotron Light Source in Barcelona in collaboration with ALBA Staff. This work is supported by the Fundação para a Ciência e Tecnologia (FCT) through the Project references: UID/Multi/04044/2013; PAMI-ROTEIRO/0328/2013 (Nº 022158), Add.Additive-POCI-01-0247-FEDER-024533 and Tailored Cooling POCI-01-0145-FEDER-03243). We thank the NM3D Iberica Company based in Marinha Grande for making the CT scans of the mould inserts

Conflict of Interests

The authors declare they have no conflicts of interests.

Data Availability Statement: The data obtained using the facilities of the ALBA Synchrotron Light Source are subject to the Generic data management policy at ALBA CELLS as can be accessed at Microsoft Word - Data_policy_Alba_v1.2_2017.doc (cells.es). The experimental data identifiers are available from the corresponding author after the end of the embargo period.

References

1. P.K. Bharti and Khan I., International Journal of Engineering Science and Technology **2010** 2(9), 4540-4554
2. Speranza, V.; Liparoti, S.; Pantani, R.; Titomanlio, G. Hierarchical Structure of iPP During Injection Molding Process with Fast Mold Temperature Evolution. *Materials* **2019**, *12*, 424. https://doi.org/10.3390/ma120304243.
3. Olley R.H., Bassett, D.C. "On the development of polypropylene spherulites", Polymer, **1989** 30(3), 399-409, doi.org/10.1016/0032-3861(89)90004-9.
4. Keller, A. and Kolnaar, H.W.H. Flow-Induced Orientation and Structure Formation. In Materials Science and Technology (eds R.W. Cahn, P. Haasen and E.J. Kramer). **2006**. https://doi.org/10.1002/9783527603978.mst0210
5. Olley, R. H. "Selective Etching of Polymeric Materials." *Science Progress* ***1986*** 70, no. 1 (277) 17–43. http://www.jstor.org/stable/43420627.
6. Mohan, S.D.; Olley, R.H.; Vaughan, A.S.; Mitchell, G.R. Evaluating Scales of Structure in Polymers, Chapter 2. In *Controlling the Morphology of Polymers: Multiple Scales of Structure and Processing* **2016** Mitchell, G., Tojeira, A., Eds.; Springer: Berlin/Heidelberg, Germany, ISBN 978-3-319-39320-9.
7. Sakurai, S., Recent developments in polymer applications of synchrotron small-angle X-ray scattering. Polym. Int. **2017** 66: 237-249. https://doi.org/10.1002/pi.5136
8. Aurora Nogales, Sarah Thornley, Geoffrey R Mitchell "Shear cell for in situ WAXS, SAXS, and SANS experiments on polymer melts under flow fields" Journal of Macromolecular Science Part B Physics **2007** 43(6):1161-1170 DOI: 10.1081/MB-200026521
9. Guruswamy Kumaraswamy and Raviraj Verma and Julia A. Kornfield and Feng-ji Yeh and Benjamin S. Hsiao "Shear-enhanced crystallization in isotactic propylene in-situ synchrotron SAXS and WAXD", Macromolecules, **2004**, 37, 9005-9017
10. Jun Fang, Wesley R. Burghardt, and Robert A. Bubeck "In Situ X-ray Scattering Measurements and Polydomain Simulations of Molecular Orientation Development during Injection Molding of Liquid Crystalline Polymers", AIP Conference Proceedings **2008** 1027, 39-41 https://doi.org/10.1063/1.2964705
11. Rendon S, Fang J, Burghardt WR, Bubeck RA. An apparatus for in situ x-ray scattering measurements during polymer injection molding. Rev Sci Instrum. **2009** Apr;80(4):043902. doi: 10.1063/1.3108531. PMID: 19405670.
12. Liao,T., Zhao, X., Yang, X., Coates, P., Whiteside, B., Barker, D., Thompson G.,, Lai, Y., Jiang, Z., Men, Y., "In situ synchrotron small angle X-ray scattering investigation of structural formation of polyethylene upon micro-injection molding" Polymer, **2021**, 215, 123390, doi.org/10.1016/j.polymer.2021.123390.
13. Zhao,Z., Liao, T., Yang, X., Coates,P., Whiteside, B., Barker,D., Thompson, G., Jiang, Z., Men, Y., "Mold temperature- and molar mass-dependent structural formation in

micro-injection molding of isotactic polypropylene", **2022** Polymer, 248, 124797, doi.org/10.1016/j.polymer.2022.124797.

14. Rai DK, Gillilan RE, Huang Q, Miller R, Ting E, Lazarev A, Tate MW, Gruner SM. High-pressure small-angle X-ray scattering cell for biological solutions and soft materials. J Appl Crystallogr. **54(1),** 111-122. doi: 10.1107/S1600576720014752. PMID: 33841059; PMCID: PMC7941318.
15. Llonch, Marta, G. Peña, Artur Gevorgyan and Yu. M. Nikitin. "NCD-SWEET BEAMLINE UPGRADE." **2018**. Online at NCD-SWEET Beamline Upgrade (cern.ch) viewed 29/8/2022
16. M Nyam-Osor *et al J. Phys.: Conf. Ser.* **2012 351** 012024
17. Rowolt, C.; Fröck, H.; Milkereit, B.; Reich, M.; Kowalski, W.; Stark, A.; Keßler, O. In-situ analysis of continuous cooling precipitation in Al alloys by wide-angle X-ray scattering. *Sci. Technol. Adv. Mater.* **2020**, 21, 205-2018. https://doi.org/10.1080/14686996.2020.1739554.
18. Olley R.H.,Mitchell G.R., and Moghaddam Y., "On row-structures in sheared polypropylene and a propylene–ethylene copolymer" European Polymer Journal **2014** 53, 37-49, doi.org/10.1016/j.eurpolymj.2014.01.010
19. Bassett, D.C., "Linear nucleation of polymers", Polymer, **2006** 47(15), 5221-5227, doi.org/10.1016/j.polymer.2006.05.028.
20. Mitchell, G.R., Saengsuwan, S., Bualek-Limcharoen, S. **2005**. Evaluation of preferred orientation in multi-component polymer systems using x-ray scattering procedures. In: Stribeck, N., Smarsly, B. (eds) Scattering Methods and the Properties of Polymer Materials. Progress in Colloid and Polymer Science, vol 130. Springer, Berlin, Heidelberg. https://doi.org/10.1007/b107341
21. Lovell, R. & Mitchell, G. R. **1981**. Acta Cryst. A37, 135-137. doi.org/10.1107/S0567739481000247